NANO LETTERS

2007
Vol. 7, No. 6
1495−1499

Metal–Molecule Interface Fluctuations

Chenggang Tao, T. J. Stasevich,† William G. Cullen, T. L. Einstein, and Ellen D. Williams*

NSF Materials Research Science and Engineering Center and Department of Physics, University of Maryland, College Park, Maryland 20742-4111

Received January 26, 2007; Revised Manuscript Received February 28, 2007

ABSTRACT

We have created self-assembled circular chains of C_{60} laterally bound to a layer of Ag atoms as a model system for characterizing fluctuations at a metal–molecule interface. STM measurements show that the Ag and C_{60} sides of the interface fluctuate independently, with frequency-dependent amplitudes of magnitude 0.1 nm at ~1 Hz for the Ag edge and ~0.01 Hz for the C_{60} ring. The measured frequency spectra of the metal and molecule fluctuation amplitudes will contribute characteristic signatures to transport measurements involving such interfaces.

Nanoscale electronics has attracted intense research interest, motivated in part by the potential use of single-molecule conduction in electronic devices.[1−3] Substantial achievements in this area make it increasingly clear that a great challenge will be understanding and controlling the interaction between the active nanoscale elements and the conductive electrodes in the devices.[4−8] Structural changes at the nanometer scale, involving the displacement of even a single metal atom, can greatly alter the electronic properties and reliability of the devices.[9−11] To shed light on this problem, we introduce a model system, a one-dimensional (1D) metal−molecule interface formed at Ag monolayer islands decorated by C_{60} molecules. Direct time-resolved imaging of this system using STM reveals the amplitude−frequency relationships for the motions of the Ag "electrode" and the C_{60} molecules at the interface.

Quantifying structural fluctuations is accomplished by using the continuum step model for interfaces to analyze time-dependent STM measurements.[12] Silver surfaces are known to display substantial structural mobility at room temperature,[13−15] resulting in correlated motion of extended structures such as pits and islands.[16−18] Carefully designed experiments allow the motion, shape, and correlation functions of the interfaces of such structures to be determined.[19−22] These reveal the time scale and amplitude of the fluctuations, which are in turn determined by the stiffness of the interface and the characteristic times for motion of the atoms at the interface.[12,23−25] More complex systems, for instance, the interfaces between molecules and metal surfaces, have not yet been investigated in this way. The adsorption of C_{60} on metal surfaces provides an ideal system for demonstrating the effects of fluctuations at a metal−molecule interface. Previous studies of C_{60} on metal surfaces have documented the characteristics of the adsorbed C_{60}, which include rapid diffusion at room temperature and preferential binding at structural edges such as steps and island boundaries.[26−29] Experimental methods for preparing the surface and methods of image analysis have been presented previously[29] and are synopsized in the Supporting Information.

At room temperature, equilibrium monolayer islands on clean Ag(111) surfaces are hexagonal.[21] The island edges appear frizzy, indicating step-edge fluctuations. Previous experimental studies have shown that the edge fluctuations at and above room temperature are dominated by diffusion of Ag atoms along the periphery of the structure.[15,21] When C_{60} molecules are deposited onto these surfaces, they bind preferentially at step edges, causing no observable change in the fluctuations of neighboring bare segments of the step edge.[29] By carefully controlling the deposition rate and time, we can generate islands with edges covered by precisely one closed single strand of C_{60}, as shown in Figure 1a. These images reveal that both adatom islands and vacancy islands (Supporting Information, Figures S1 and S2) are covered by closed C_{60} chains one molecule wide, which we call C_{60} rings. In these images, we can also clearly see that the shape of the decorated islands larger than 20 nm is approximately circular. On closer inspection (Supporting Information, Figure S2c), the C_{60} rings are not smooth circles with constant local curvature; some sections have higher curvature than others, and there are some tortuous structures indicating kinked configurations. Furthermore, as shown in Figure 1b,c, the images of some C_{60} molecules in the rings appear disjointed, indicating C_{60} molecules have moved between sequential scans. The temporal signature of such motion is illustrated in Figure 1d. On the whole, the shape of the C_{60} ring fluctuates visibly on the time scale of sequential STM

* Corresponding author. E-mail: edw@umd.edu.
† Present address: Fluorescence Imaging Facility, Laboratory of Receptor Biology and Gene Expression, National Cancer Institute, NIH, Bethesda, MD 20892.

10.1021/nl070210a CCC: $37.00
Published on Web 03/13/2007

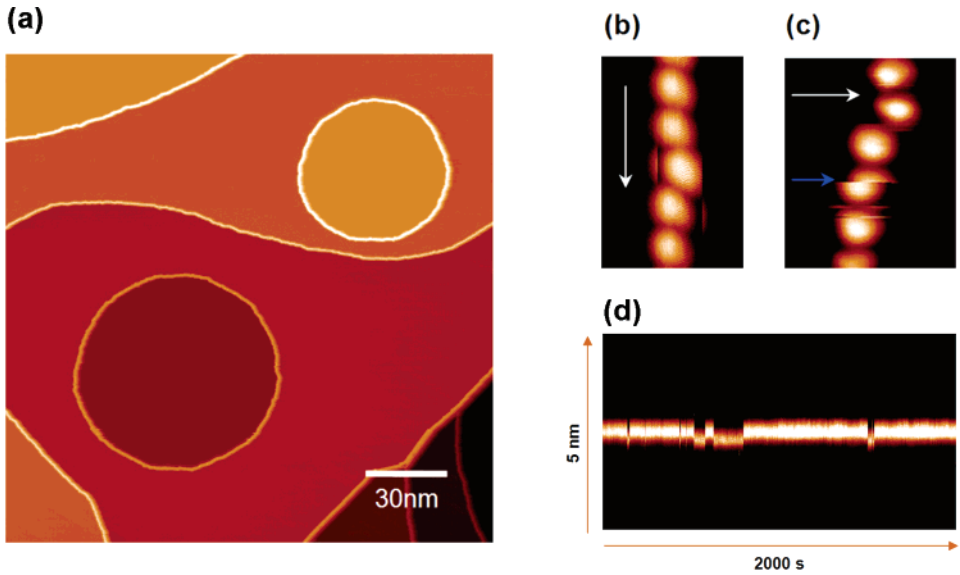

Figure 1. (a) STM topography images of Ag islands decorated by closed C_{60} chains. The tunneling conditions are $U_{sample} = -1.71$ V and $I_t = 86$ pA. (b and c) STM images showing C_{60} displacements between sequential scans. White arrows indicate scan direction. (d) Temporal STM image of an individual C_{60} molecule in the C_{60} chains hopping. The STM tip repeatedly scans over the top of a single C_{60} molecule, as noted by the blue arrow in (c). The time intervals between observed hopping events are from 6.1 to 170.8 s, and the displacement of the C_{60} molecule along the scan direction is 0.263 nm. The scan direction is 17° from the close-packed direction of the substrate, and the lattice constant of Ag(111) is 0.289 nm. Thus the C_{60} motion is consistent with a hop from a stable position to a nearest-neighboring stable position.

images, with a time scale substantially slower than the edges of undecorated Ag islands on clean Ag(111) surfaces.

Because the C_{60} rings are fluctuating at room temperature, we use STM to repeatedly scan relatively small decorated islands, as shown in Figure 2a, to obtain a temporal sequence of images (Supporting Information Movie S3). The images are then processed to determine molecular positions, and one frame of such an STM image ensemble is shown in Figure 2b, in which the blue dots represent the STM topography image of C_{60} molecules, and the orange dots are the digitized C_{60} positions. Both the island area and the number of C_{60} molecules in the surrounding C_{60} ring remain constant over the entire sequence of images, with total measurement time around 60 min. By averaging the images in a sequence, we obtain the mean shape of the decorated island (or the C_{60} ring), the equilibrium shape,[30] as shown in Figure 2c. Distinctly different from the hexagonal shape of bare Ag islands, the equilibrium shape of the decorated island is almost perfectly circular, with an average $C_{60}-C_{60}$ distance close to 1 nm. Such circular structures are expected to fluctuate in the normal modes of a circle, as illustrated schematically in Figure 2d. To obtain the kinetic properties of the decorated island, many sequential images are needed for longer total measurement time and a shorter time interval for higher time resolution. To address these requirements, we analyzed a data set for a decorated island by a ring including $N = 78$ C_{60} molecules. The ensemble includes ~600 sequential images with a time interval of 13.1 s for a total measurement time around 130 min. To determine the structural correlation functions, the edge of the ring is approximated by a series of measurements of the radius $R(\theta_n)$ at equally spaced angles, where $\theta_n = 2n\pi/N$ with $N = 78$, the number of C_{60} in the ring. To analyze the fluctuations, we subtract the equilibrium circular shape from each digitalized island shape, leaving a new series $r(\theta_n) = R(\theta_n) - \langle R \rangle$, where $\langle R \rangle$ is the radius of the equilibrium circle.

Given $r(\theta_n)$, we Fourier transform to determine the magnitudes r_k of the component Fourier modes:

$$r_k = \frac{1}{N} \sum_{n=-N/2+1}^{N/2} r(\theta_n)\, e^{ik\theta_n} \qquad (1)$$

Once we know r_k, it is straightforward to calculate correlation functions in the Fourier representation:[23,24]

$$G_k(t) = \langle [r_k(t + t_0) - r_k(t_0)]^2 \rangle = A_k(1 - e^{-t/\tau_k}) \qquad (2)$$

where A_k is the mean squared amplitude of the radial fluctuations in the kth mode, and τ_k is the time constant for the kth mode. The correlation functions for modes 2−12 are plotted in Figure 3a. Fitting the correlation functions to eq 2 yields the parameters A_k and τ_k.

Both the amplitude and the time constant are expected to have a power-law dependence on the mode number k. Hence, we plot A_k vs k and τ_k vs k in Figure 3b. We find the scaling relationship $A_k = (0.108 \pm 0.002) \times k^{-\alpha}$ nm^2 with $\alpha = 1.88 \pm 0.01$, consistent with the prediction of the Langevin analysis:

$$A_k = \frac{k_B T \langle R \rangle}{\pi \tilde{\beta} k^2} \qquad (3)$$

where $\tilde{\beta}$ is the decorated-edge stiffness. From eq 3, we determine $\tilde{\beta} = 0.65$ eV/nm. According to our previous

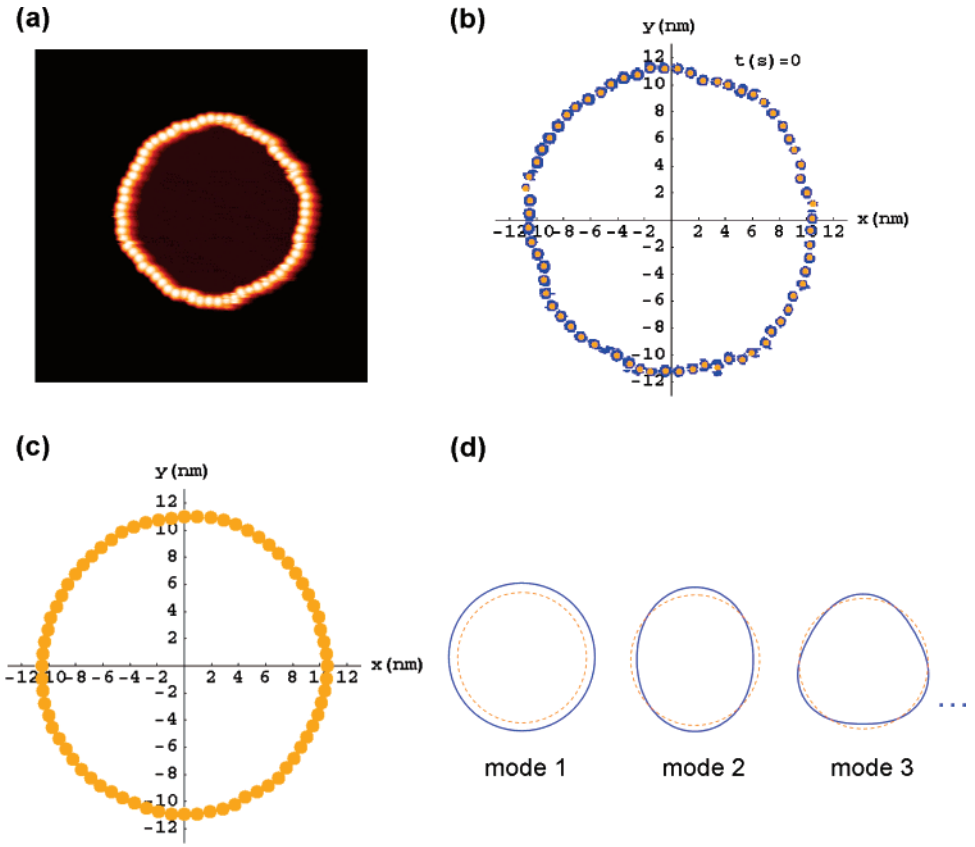

Figure 2. (a) STM topography of a C_{60} ring covering the Ag island edge, obtained from one frame of a set of 66 sequential images measured with time interval 52.4 s. (b) The large blue dots represent areas of bright contrast due to C_{60} of the STM topography image, and the orange dots are digitized positions of each C_{60}. See Supporting Information for time-lapse movie (S3) showing fluctuations. (c) The mean shape of the C_{60} ring by averaging over 66 sequential topography STM images. (d) Schematic of circular fluctuation modes.

study,[15] the edge stiffness of bare steps on Ag(111) at room temperature depends on step orientation. For steps deviating from the close-packed direction, the average experimental step stiffness is 0.67 eV/nm,[29,31] which is similar to the above decorated-edge stiffness. On the other hand, Figure 3b shows the scaling relationship $\tau_k \propto k^{-z}$ with $z = 1.85 \pm 0.05$, indicating that the decorated-island shape fluctuations follow the behavior expected for uncorrelated motion ($z = 2$, usually attributed to attachment−detachment (AD) kinetics). This is in stark contrast to the correlated motion of Ag atoms on the bare Ag(111) step boundary, characterized by a $z = 4$ power law for the temporal fluctuations.

The scaling behavior of τ_k suggests that the fluctuations of the 1D Ag−C_{60} interface are governed by uncorrelated events, similar to the behavior observed for attachment−detachment kinetics at step edges. However, in this case, the observed invariance of number of C_{60} molecules is inconsistent with exchange of C_{60} molecules between the ring and a diffuse phase beyond the decorated-island edges. Instead, the observed structural configurations suggest uncorrelated C_{60} displacements within the ring, most likely involving molecular displacements as shown in Figure 1b,c. These quasikink local configurations are related to C_{60} molecules in the rings hopping approximately along the radial direction to a nearest stable position. This idea is confirmed by temporal line scans over individual C_{60} molecules (Figure 1d). The displacements occur only between two discrete positions. The hopping displacement of 0.26 nm suggests registry to the underlying Ag lattice.

The distinct difference in the basic nature of the fluctuations of the underlying Ag side of the interface and the directly observed C_{60} ring indicate that motion of the C_{60} side of the interface is not strongly coupled to the underlying Ag motion. For the C_{60} ring fluctuations, using the theoretical values $\alpha = 2$ and $z = 2$, we obtain mode k and radius R dependence of A_k and τ_k: $A_k = (0.009\ \text{nm})(R/k^2)$ and $\tau_k = (11.5\ \text{nm}^{-2}\ \text{s})(R/k)^2$. In comparison, for bare Ag step edges, for which previously determined values for the step stiffness and hopping time constant are available,[15] the corresponding relationships are $A_q = 2k_BT/L\tilde{\beta}q^2$ and $\tau_q = k_BT/\Gamma_h\tilde{\beta}q^4$, respectively, where L is the system length and q is the wavenumber.[12] If step edges are considered as closed interfaces, we can equate the system length with the perimeter of the circular boundary, unifying the formulas for both step edges and islands. Because $L = 2\pi R = k\lambda$ and $q = 2\pi/\lambda = k/R$, then the squared-amplitude A_q and the time constant τ_q can be represented in terms of the mode number k as $A_k = k_BTR/\pi\tilde{\beta}k^2$ and $\tau_k = k_BTR^4/\Gamma_h\tilde{\beta}k^4$. The resulting formula for A_k for step edges is identical to eq 3. From our previous study,[29] the step mobility is $\Gamma_h = 2.86\ \text{nm}^5\ \text{s}^{-1}$, so for bare step edges around a circular boundary of radius R, $A_k = (0.012\ \text{nm})(R/k^2)$ and $\tau_k = (0.0135\ \text{nm}^{-4}\ \text{s})(R/k)^4$. Physical examples of the resulting time constant values for mode 4 are, for bare step edges, $\sqrt{A_4} = 0.09$ nm and τ_4

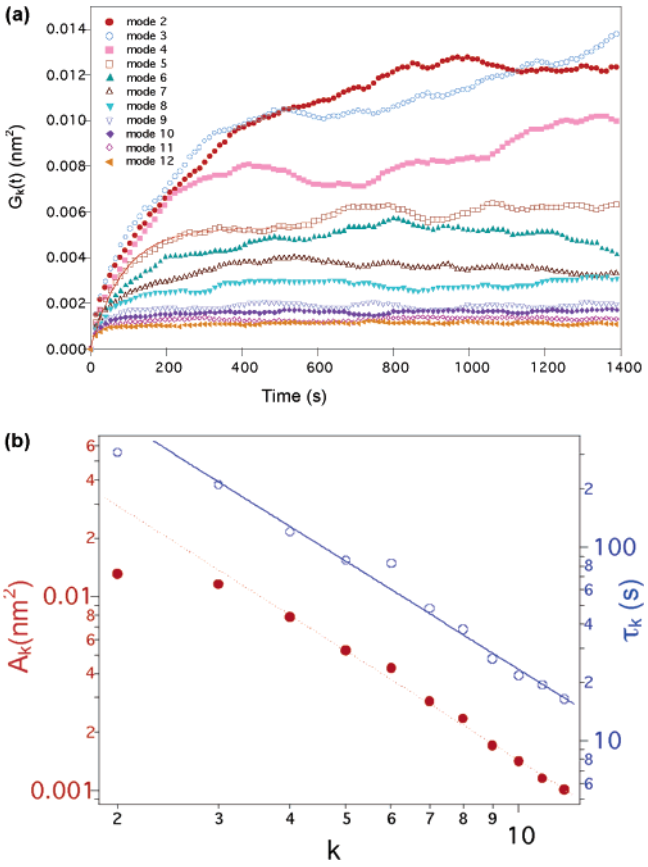

Figure 3. (a) Correlation functions for different modes of the ring shape fluctuation. The solid red curve is the corresponding fit to eq 2 for mode 5. (b) A_k and τ_k vs k. The dashed red line is the power law fitting for the experimental data, $A_k = A_0 \times k^{-\alpha}$. The best fit is $A_0 = 0.108 \pm 0.002$ nm^2, and $\alpha = 1.88 \pm 0.01$. The solid blue line is the power law fitting for the experimental data, $\tau_k = \tau_0 \times k^{-z}$. The best fit is $\tau_0 = 1660 \pm 145$ s, and $z = 1.85 \pm 0.05$.

$= 0.8$ s, while for Ag−C_{60} interfaces, $\sqrt{A_4} = 0.08$ nm and $\tau_4 = 120$ s. Compared with the effects of Ag atoms hopping along bare Ag step edges, the mode motion resulting from C_{60} molecular displacements is a slow process. Previous measurements of partially covered Ag steps have shown that the C_{60} molecules attached to island edges do not alter the Ag step fluctuations. This strongly suggests that in this system the underlying Ag step edge is fluctuating with at most weak correlation with the motion of the C_{60} overlayer. In this case, the independent motions of the Ag and the C_{60} will contribute to the electronic properties of the interface by creating fluctuations of the Ag−C_{60} separation, introducing signal variability with an amplitude spectrum ($T = 300$ K) combining the silver signature $A_k(f_k = 1/\tau_k) = 0.10$ nm$^3/R\, f_k^{-1/2}$ and the C_{60} signature $A_k(f_k = 1/\tau_k) = (8 \times 10^{-4}$ nm$^3)/R\, f_k^{-1}$. The effect on electron transport signals will be strongest where the amplitudes are largest, e.g., in the frequency range (modes 4−12) of 1.3−105 Hz due to Ag motion and 0.01−0.08 Hz due to C_{60} motion.

The ability to structure C_{60} molecules into rings decorating Ag islands provides a model system in which the observable collective fluctuations of the metal−molecule interface can be readily interpreted in terms of fundamental time constants and free energies. It is shown here that the C_{60} rings decorating Ag islands provide a model to study the organic molecule−metal interface fluctuations. By analyzing the interface fluctuations, we obtain time constants corresponding to frequencies of 0.01−100 Hz and an amplitude for changes in the interface width of ∼0.1 nm. Such interface fluctuations will directly impact the transport properties of nanoelectronic and molecular electronic devices that involve small area contacts between electrodes and the electronic material.[11] The approach presented here provides a quantitative method for characterizing the stochastic properties of electronic interfaces on the nanometer scale and predicting the correlated frequency spectrum of the signature in electrical transport across the interface.

Acknowledgment. This work has been supported by the NSF-MRSEC at University of Maryland under grant DMR 05-20471. The NSF-MRSEC SEF were used in obtaining the data presented.

Supporting Information Available: Detailed experimental procedures (PDF); movie of a STM image ensemble including 66 sequential images with time interval 52.4 s (AVI). This material is available free of charge via the Internet at http://pubs.acs.org.

References

(1) Aviram, A.; Ratner, M. A. *Chem. Phys. Lett.* **1974**, *29*, 277−283.
(2) Tans, S. J.; Verschueren, A. R. M.; Dekker, C. *Nature* **1998**, *393*, 49−52.
(3) Park, H.; Park, J.; Lim, A. K. L.; Anderson, E. H.; Alivisatos, A. P.; McEuen, P. L. *Nature* **2000**, *407*, 57−60.
(4) Zhirnov, V. V.; Cavin, R. K. *Nat. Mater.* **2006**, *5*, 11−12.
(5) Guo, X. F.; Small, J. P.; Klare, J. E.; Wang, Y. L.; Purewal, M. S.; Tam, I. W.; Hong, B. H.; Caldwell, R.; Huang, L. M.; O'Brien, S.; Yan, J. M.; Breslow, R.; Wind, S. J.; Hone, J.; Kim, P.; Nuckolls, C. *Science* **2006**, *311*, 356−359.
(6) Kushmerick, J. G.; Blum, A. S.; Long, D. P. *Anal. Chim. Acta* **2006**, *568*, 20−27.
(7) Garner, C. M.; Vogel, E. M. *IEEE Trans. Semicond. Manuf.* **2006**, *19*, 397−403.
(8) Haiss, W.; Wang, C.; Grace, I.; Batsanov, A. S.; Schiffrin, D. J.; Higgins, S. J.; Bryce, M. R.; Lambert, C. J.; Nichols, R. J. *Nat. Mater.* **2006**, *5*, 995−1002.
(9) Di Ventra, M.; Pantelides, S. T.; Lang, N. D. *Phys. Rev. Lett.* **2000**, *84*, 979−982.
(10) Yu, L. H.; Zangmeister, C. D.; Kushmerick, J. G. *Nano Lett.* **2006**, *6*, 2515−2519.
(11) Basch, H.; Cohen, R.; Ratner, M. A. *Nano Lett.* **2005**, *5*, 1668−1675.
(12) Jeong, H. C.; Williams, E. D. *Surf. Sci. Rep.* **1999**, *34*, 175−294.
(13) Frenken, J. W. M.; Hamers, R. J.; Demuth, J. E. *J. Vac. Sci. Technol., A* **1990**, *8*, 293−296.
(14) Poensgen, M.; Wolf, J. F.; Frohn, J.; Giesen, M.; Ibach, H. *Surf. Sci.* **1992**, *274*, 430−440.
(15) Bondarchuk, O.; Dougherty, D. B.; Degawa, M.; Williams, E. D.; Constantin, M.; Dasgupta, C.; Das Sarma, S. *Phys. Rev. B* **2005**, *71*, 045426.
(16) Morgenstern, K.; Rosenfeld, G.; Comsa, G. *Phys. Rev. Lett.* **1996**, *76*, 2113−2116.
(17) Schlosser, D. C.; Verheij, L. K.; Rosenfeld, G.; Comsa, G. *Phys. Rev. Lett.* **1999**, *82*, 3843−3846.
(18) Wen, J. M.; Chang, S. L.; Burnett, J. W.; Evans, J. W.; Thiel, P. A. *Phys. Rev. Lett.* **1994**, *73*, 2591−2594.
(19) Bartelt, N. C.; Tromp, R. M.; Williams, E. D. *Phys. Rev. Lett.* **1994**, *73*, 1656−1659.

(20) Rost, M. J.; van Albada, S. B.; Frenken, J. W. M. *Phys. Rev. Lett.* **2001**, *86*, 5938−5941.
(21) Giesen, M.; Steimer, C.; Ibach, H. *Surf. Sci.* **2001**, *471*, 80−100.
(22) Schmid, A. K.; Bartelt, N. C.; Hwang, R. Q. *Science* **2000**, *290*, 1561−1564.
(23) Khare, S. V.; Einstein, T. L. *Phys. Rev. B* **1996**, *54*, 11752−11761.
(24) Szalma, F.; Gebremariam, H.; Einstein, T. L. *Phys. Rev. B* **2005**, *71*, 035422.
(25) Khare, S. V.; Kodambaka, S.; Johnson, D. D.; Petrov, I.; Greene, J. E. *Surf. Sci.* **2003**, *522*, 75−83.
(26) Altman, E. I.; Colton, R. J. *Phys. Rev. B* **1993**, *48*, 18244−18249.
(27) Lu, X.; Grobis, M.; Khoo, K.; Louie, S.; Crommie, M. *Phys. Rev. Lett.* **2003**, *90*, 096802.
(28) Hashizume, T.; Motai, K.; Wang, X. D.; Shinohara, H.; Saito, Y.; Maruyama, Y.; Ohno, K.; Kawazoe, Y.; Nishina, Y.; Pickering, H. W.; Kuk, Y.; Sakurai, T. *Phys. Rev. Lett.* **1993**, *71*, 2959−2962.
(29) Tao, C.; Stasevich, T. J.; Einstein, T. L.; Williams, E. D. *Phys. Rev. B* **2006**, *73*, 125436.
(30) Stasevich, T. J.; Tao, C. G.; Cullen, W. G.; Einstein, T. L.; Williams, E. D. **2006**, in preparation.
(31) Stasevich, T. J.; Gebremariam, H.; Einstein, T. L.; Giesen, M.; Steimer, C.; Ibach, H. *Phys. Rev. B* **2005**, *71*, 245414.
(32) Baski, A. A.; Fuchs, H. *Surf. Sci.* **1994**, *313*, 275−288.
(33) Levlin, M.; Laakso, A. *Appl. Surf. Sci.* **2001**, *171*, 257−264.

NL070210A